

ULRR

Active cooling of a mobile phone handset

| | |
|---------------|---|
| Item Type | Article |
| Authors | Grimes, Ronan;Walsh, Ed J.;Walsh, Pat A. |
| Citation | Applied Thermal Engineering;30(16), November, pp. 2363-2369 |
| Publisher | Elsevier |
| Download date | 2026-03-14 22:22:47 |
| Item License | https://creativecommons.org/licenses/by-nc-sa/1.0/ |
| Link to Item | https://hdl.handle.net/10344/2398 |

Accepted Manuscript

Title: Active Cooling Of A Mobile Phone Handset

Authors: Ronan Grimes, Ed Walsh, Pat Walsh

PII: S1359-4311(10)00249-8

DOI: [10.1016/j.applthermaleng.2010.06.002](https://doi.org/10.1016/j.applthermaleng.2010.06.002)

Reference: ATE 3133

To appear in: *Applied Thermal Engineering*

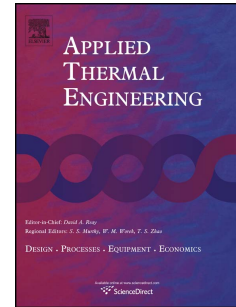
Received Date: 10 July 2009

Revised Date: 31 May 2010

Accepted Date: 1 June 2010

Please cite this article as: R. Grimes, E. Walsh, P. Walsh. Active Cooling Of A Mobile Phone Handset, *Applied Thermal Engineering* (2010), doi: 10.1016/j.applthermaleng.2010.06.002

This is a PDF file of an unedited manuscript that has been accepted for publication. As a service to our customers we are providing this early version of the manuscript. The manuscript will undergo copyediting, typesetting, and review of the resulting proof before it is published in its final form. Please note that during the production process errors may be discovered which could affect the content, and all legal disclaimers that apply to the journal pertain.



ACTIVE COOLING OF A MOBILE PHONE HANDSET

Ronan Grimes, Ed Walsh, Pat Walsh

Stokes Institute,

University of Limerick,

Limerick

Ireland

Phone: +353 61 213181

Fax: +353 61 202393

Email: edmond.walsh@ul.ie

ABSTRACT

Power dissipation levels in mobile phones continue to increase due to gaming, higher power applications, and increased functionality associated with the internet. The current cooling methodologies of natural convection and radiation limit the power dissipation within a mobile phone to between 1-2 W depending on size. As power dissipation levels increase, products such as mobile phones will require active cooling to ensure that the devices operate within an acceptable temperature envelope from both user comfort and reliability perspectives. In this paper, we focus on the applied thermal engineering problem of an active cooling solution within a typical mobile phone architecture by implementing a custom centrifugal fan within the mobile phone. Its performance is compared in terms of flow rates and pressure drops, allowable phone heat dissipation and maximum phone surface temperature as this is the user constraint for a variety of simulated PCB architectures in the mobile phone. Perforated plates with varying porosity through different size orifices are used to simulate these architectures. The results show that the power level dissipated by a phone for a constant surface temperature may be increased by ~50 - 75% depending on pressure drop induced by the internal phone architecture. Hence for successful implementation and efficient utilization of active cooling will require chip layout to be considered at the design stage.

KEY WORDS: mobile phone, active cooling, portable electronics, fan, forced convection.

NOMENCLATURE

| Symbol | Description | Unit |
|------------|---|---------------------------------|
| A | Area | m ² |
| e | Estimated error in allowable heat dissipation | % |
| g | Acceleration due to gravity | m/s ² |
| Gr | Grashof number | - |
| h | Heat transfer coefficient | W/m ² K |
| k | Thermal conductivity | W/mK |
| L | Length | m |
| Nu | Nusselt number | - |
| Pr | Prandtl number | - |
| \dot{Q} | Heat dissipation | W |
| R | Thermal resistance | °C/W |
| T | Temperature | °C |
| β | Coefficient of volume expansion | °C ⁻¹ |
| ΔT | Temperature difference | °C |
| ν | Kinematic viscosity | m ² /s |
| σ | Stefan Boltzmann constant | W/m ² K ⁴ |
| ϵ | Emissivity | - |

Subscripts

| Symbol | Description |
|--------|--|
| A | Conditions of maximum allowable case to ambient temperature difference |
| c | Phone case |
| c – ∞ | Case to ambient |
| FC | Forced convection |
| h – ∞ | Heater to ambient |
| NC | Natural convection |
| PCB | Printed circuit board |
| R | Radiation |
| T | Total heater to ambient quantity |
| t | Quantity under test conditions |
| ∞ | Ambient |

INTRODUCTION

The mobile phone market continues to ship vast quantities, in the hundreds of millions, each year. As users continue to demand more functionality, and small size the issues of cooling become more critical. The thermal design of any electronic system is undertaken to meet the

system operating thermal constraints. For the case of the mobile phone in particular, user comfort requires case temperature to be typically less than fifty degrees Celsius, which requires that the phone to ambient temperature difference is typically of the order of fifteen degrees Celsius. To achieve a satisfactory thermal management solution a number of cooling methodologies can be implemented and are dependant upon a number of factors, which include the level of heat to be dissipated, the operating environment, the maximum allowable component temperatures, the available space, acoustic levels, reliability and ultimately cost. From a cooling perspective a fundamental challenge in the mobile phone market place is the consumer demand for low profile, pocket sized devices. This has many new challenges, whereas in traditional active cooling in desktop computers can employ relatively large scale heat sinks and fans, and may be used to directly cool heat generating components as space is not assigned a high value. Even in the laptop fans are typically around fifteen millimeters, or greater in height. The use of large scale fans and heat sinks results in high heat transfer coefficients, particularly when mounted directly on the components to be cooled. Much work has been done in recent years to characterize and optimize the performance of fan heat sink modules, Lin and Chou [1] and Loh, *et al.* [2] are examples. However this work has focused on large scale applications, with little effort, to date, focused on scales appropriate to handheld electronic devices such as mobile phones. For low profile scales the design of cooling solutions becomes more difficult and new ideas and approaches should be considered. Examples of technologies under development for thermal management of portable electronic devices are phase change materials Tan and Tso [3], micro heat pipes Launay, *et al.* [4] and high conductivity materials such as carbon substrates. The focus of these technologies is upon heat spreading and transport within a device rather than active removal of heat from the device. For example, the phase change materials store heat to be dissipated over time, while liquid cooling, heat pipes and high conductivity materials only provide paths of reduced thermal resistance to the flow of heat within devices. Hence, heat is ultimately removed by some combination of natural convection, conduction and radiation. Novel, low profile finless heat sink designs with active cooling and heights of less than five millimeters have been studied in terms of heat sink designs by Walsh *et al.* [5], Walsh and Grimes [6], and the importance of flow field at the exit of small scale fans of low profile, Egan *et al.* [7,8] and the position of chip placement in the case of axial flow fans, Stafford *et al.* [9].

Currently the larger scale phone and palm computer devices typically have dimensions of 100, 80 and 20 mm for length, width and depth respectively. Using this surface area combined with the assumptions of an isothermal surface with an allowable temperature rise above ambient of 15 °C (45 °C in 30 °C environment) and an average heat transfer coefficient of 8 W/m²K, the maximum power dissipated would be around 2 W, the value being about 1 W for smaller phones such as that investigated here. Importantly the isothermal phone is not a reality and hence the actual cooling potential is reduced further for the more realistic non isothermal handset. Given that many such devices are striving towards laptop performance which dissipates several multiples of the mobile phone power levels, it is clear that thermal management of such devices is impeding the enhancement of performance and the need for active cooling solutions is evident. Recently, studies addressing the effects of geometrical scaling in both axial and radial fans has provided guidelines for some of the limitation of low profile fans in terms of aerodynamics, Grimes, *et al.* [10] and Walsh, *et al.* [11], and acoustics by Walsh *et al.* [12] to the development of low profile fans for potential use in small scale electronics cooling applications.

This short paper addresses the applied problem of integration of a custom designed fan technology into low profile portable electronics. Previous work by Walsh *et al* [13] was limited to thermal measurements only, and this work provides a more complete analysis which can be used for benchmarking of numerical models. The fan is firstly aerodynamically characterized. It is then integrated within handset architectures and its performance is characterized in terms of flow rate, pressure drop and temperature rise above ambient. This results in estimation of the increased power dissipation that is possible through implementation of fans in handsets. Various chip layout configurations are simulated through different levels of blockage in the phone using perforated plates with varying porosity. This is important, as all layout configurations are different and the methodology taken herein is not specific to any particular phone architecture. The results show that the power level dissipated by a phone for a constant surface temperature may be increased by ~50 - 75% depending on pressure drop induced by the internal phone architecture. The importance of reducing fan rotational speed to conserve battery power is also highlighted.

EXPERIMENTAL

A Nokia 3120 illustrated in figure 1 was used as the handset to perform the experimental tests. This phone has external dimensions of 102x43x20 mm. Figure 2(a) shows a populated PCB within the phone. In the original form of the phone these components faced towards the battery at the back of the phone, and were covered by the metal sheet also shown in figure 2(a). In order to provide space for the inclusion of a fan and a heater, all the components on this PCB, and the metal cover sheet were removed, and the heater and fan were placed on the PCB as illustrated in figure 2(b). The heater enabled the dissipation of a known power level in the phone. Figure 2(c) schematically illustrates the layout of the phone, showing the location of inlet and outlet vents which were machined into the casing of the phone, and the positions of the fan, heater and battery.

To assess the effects of blockage on the performance of the fans, varying degrees of blockage were placed in the flow path. These blockages were provided by perforated plates spanning the width of the phone, and the height of the gap between the PCB and the back cover, downstream of the fan, as illustrated in figure 2(c). The perforations took the form of eight holes, spaced 8mm apart across the width of the plate. To vary the degree of the blockage, holes of diameter 1, 1.6 and 2.5 mm were used.

The fan which was custom designed and manufactured to cool the phone is illustrated in figure 2(b). This fan has dimensions of 24 x 23 x7 mm. With a volume of approximately 2.5 cc the fan occupies approximately 2.8% of the volume of the phone. When operated at 4,000 RPM the fan consumed approximately 26 mW, approximately 1.3% of the typical maximum power consumption of a phone of the type investigated here. Measurements of acoustic noise were not performed in this investigation, however Walsh *et al* 2009[12] measured equivalent sound levels of 27 and 35 dBA for a fan of similar design and diameter at speeds of 4000 and 7500 RPM respectively at five centimeters distance from the fan inlet. This sound level is low enough not to affect call quality, and moreover the fan would typically only operate when the mobile phone is performing power hungry applications such as gaming or internet usage; in both instances the user would be at a much greater distance than five centimeters.

To determine the aerodynamic characteristics of the fan, it was tested in the authors' fan performance characterization facilities described by Grimes et al. [8]. These measurements are presented in the results and discussion section. To prevent recirculation of flow from the fan outlet to the fan inlet a gasket was placed at the fan inlet as illustrated in figure 2(c). Initial tests performed in the absence of this gasket showed significantly higher thermal resistances than in the presence of the gasket, and highlighted the importance of prevention of recirculation from fan outlet to fan inlet.

Temperature measurements were performed using thermocouples mounted on the front and back surfaces of the phone. These were located at the points of maximum temperature on each surface, as identified from IR images of the surfaces of the phone. Such an IR image is illustrated in figure 3. On the front cover, the thermocouple was located 42 mm from the base of the phone on the centre line of the phone. On the back cover, the thermocouple was located 46 mm from the base of the phone, again on the centre line. Ambient temperature was also monitored using a thermocouple. A thermocouple was also located on the PCB at the location indicated in figure 2(b) All thermocouples were connected to a Labview data logging system. All temperatures were recorded under steady state conditions. The heat dissipated by the heater was set at 2 W. To minimize the effects of external air currents on the heat dissipated by the phone, the phone was placed in an enclosure measuring approximately 0.5x0.5x0.5 m.

Table 1 describes the range of phone configurations which were investigated. These configurations will be referred to by the number designated here henceforth. In all configurations the heater power is set at 2 W. Configuration 1 has no active cooling. Configuration 2 is cooled by the fan at 7500 RPM. Configurations 3 to 5 are also cooled by the fan at 7500 RPM, but with increasing levels of blockage. Configuration 6 is cooled by the fan at 4000 RPM, with a perforated plate with 1.6mm holes.

In the results and discussion section the data is presented in terms of the temperature rise of the phone above ambient ($\Delta T_{c-\infty}$) per unit heat dissipated by the heater (\dot{Q}_t). The other measure of the performance of the cooling solutions is the heat which may be dissipated by the phone (\dot{Q}_A)

for a given allowable surface temperature rise ($\Delta T_{c-\infty_A}$) of the phone's casing above ambient.

This is defined as:

$$\dot{Q}_A = \dot{Q}_t \frac{\Delta T_{c-\infty_A}}{\Delta T_{c-\infty_t}} \quad (1)$$

where $\Delta T_{c-\infty_t}$ is the maximum measured surface temperature rise above ambient of the phone for a heat dissipation of \dot{Q}_t . The maximum allowable temperature rise above ambient for the surface of a handheld device is typically regarded to be 15 °C, and this is the value of $\Delta T_{c-\infty_A}$ used here. As will be shown in the next subsection, testing the phone at case temperatures other than the allowable case temperature causes a variation in case to ambient thermal resistance, and therefore results in a small error in the allowable heat dissipation estimated by eq. 1.

Influence of case temperature on quantification of allowable heat dissipation

The flow of heat within the handset from source to ambient may be represented in a simplified manner by the thermal resistance network illustrated in figure 4. There are two primary heat flow paths, as follows:

- Passive dissipation, \dot{Q}_C : conduction from heater to case, and natural convection and radiation from case to ambient
- Forced dissipation, \dot{Q}_{FC} : forced convection from the heated surfaces directly into the forced air stream

As discussed above, the tests in this investigation were performed at a fixed total heat dissipation, \dot{Q}_t of 2 W, and the allowable heat dissipation was calculated based on the assumption of fixed case to ambient thermal resistance. However, because the case to ambient thermal resistance is the result of a natural convection component and a radiation component, its value varies with case temperature. In the tests which were performed, the maximum case to ambient temperature difference was at all times greater than the allowable value, $\Delta T_{c-\infty_A}$. Therefore, under test conditions, the case to ambient thermal resistance was lower than it would be under allowable conditions, and the allowable heat transfer as calculated using eq. 1 is over estimated by a small amount. To estimate the error associated with eq. 1 caused by this effect, eq. 2 was derived from a simple analysis of the thermal resistance network presented in figure

4. Unlike eq. 1, eq. 2 takes account of the variation in case to ambient thermal resistance with varying case to ambient temperature difference.

$$Q_A = \dot{Q}_t \left(\frac{\Delta T_{c-\infty_A}}{\Delta T_{c-\infty_t}} \right) \left(\frac{R_{FC} R_{c-\infty_t} \Delta T_{c-\infty_t}}{R_{c-\infty_A} (\Delta T_{c-\infty_t} R_{FC} + \Delta T_{h-\infty_t} R_{c-\infty_t}) - Q_t (R_{T_A} R_{c-\infty_A} R_{c-\infty_t})} \right) \quad (2)$$

Where the total heater to ambient thermal resistance under conditions of $\Delta T_{c-\infty_A}$ can be evaluated from:

$$R_{T_A} = \frac{R_{FC} (R_{PCB} + R_{c-\infty_A})}{R_{FC} + R_{PCB} + R_{c-\infty_A}} \quad (3)$$

Therefore, by combining eq. 1 and 2, the percentage error incurred through the assumption of fixed case to ambient thermal resistance may be estimated from eq. 4 as:

$$e = \left[1 - \frac{R_{FC} R_{c-\infty_t} \Delta T_{c-\infty_t}}{R_{c-\infty_A} (\Delta T_{c-\infty_t} R_{FC} + \Delta T_{h-\infty_t} R_{c-\infty_t}) - Q_t (R_{T_A} R_{c-\infty_A} R_{c-\infty_t})} \right] \times 100 \quad (4)$$

As $\Delta T_{c-\infty_t}$ approaches $\Delta T_{c-\infty_A}$, $R_{c-\infty_t}$ approaches $R_{c-\infty_A}$ and the error approaches zero.

As defined in eq. 4, the case to ambient thermal resistance is a function of the radiative and convective heat transfer coefficients, and so for each configuration the case to ambient thermal resistance was calculated from:

$$R_{c-\infty} = \frac{1}{(h_r + h_{NC})A} \quad (5)$$

The radiative heat transfer coefficient may be calculated from eq. 6 [14]:

$$h_r = \epsilon_c \sigma (T_c^2 + T_\infty^2) (T_c + T_\infty) \quad (6)$$

And the convective heat transfer coefficient may be calculated from [14]:

$$h_{NC} = \frac{k}{L} C (Gr Pr)^m \quad (7)$$

The values used for C and m were 0.53 and 0.25 respectively. The Grashof number may be calculated from:

$$Gr = \frac{g \beta \Delta T_{c-\infty} L^3}{\nu^2} \quad (8)$$

The PCB thermal resistance, which was assumed not to vary between configurations, was calculated using measured values from configuration 1. As no heat was dissipated through forced convection in this configuration, the total thermal resistance in configuration 1 was assumed to be the sum of the PCB resistance, R_{PCB} , and the case to ambient thermal resistance, $R_{c-\infty}$. Using the measured case temperature and eq. 5 to 8, $R_{c-\infty}$ was calculated. The total thermal resistance was calculated by dividing the heater to ambient temperature difference by the heater power. R_{PCB} was then calculated from $R_T - R_{c-\infty}$. This value of R_{PCB} was subsequently used for all other configurations. The forced convection thermal resistance for configurations 2 to 6 was calculated from:

$$R_{FC} = \frac{R_{T_i} (R_{PCB} + R_{c-\infty_i})}{R_{PCB} + R_{c-\infty_i} - R_{T_i}} \quad (9)$$

Again, the case to ambient thermal resistance, $R_{c-\infty_i}$ was calculated for each of these configurations using measured case and ambient temperatures, and eq. 5 to 8. The total thermal resistance from heater to ambient under test conditions (R_{T_i}) was found using the measured heater and ambient temperatures and the heater power.

Table 2 lists the values which were used in eq. 3 to 9 in order to evaluate e for configurations 1 and 3. These configurations had the highest and lowest values of e respectively. Table 1 also shows the estimated error to vary from 9% for configuration 1 to 0% for configuration 3. It should be noted that the error which is calculated through this analysis is only approximate due to the simplifications involved in the thermal resistance network coupled with difficulties in quantifying the emissivity of the casing of the phone and difficulty in defining nodal temperatures, particularly the case node temperature as the case is highly non-isothermal. However the implication of this analysis is that the over estimation of allowable heat dissipation is greatest for configuration 1, and the over estimation reduces as the fan induced flow rate is increased.

RESULTS AND DISCUSSION

Figure 5 presents the measured performance characteristics for the fan at 7500 RPM. Here it is seen that the fan has a zero flow pressure rise of approximately 19 Pa, and a zero pressure rise flow rate of approximately $0.00018 \text{ m}^3/\text{s}$. These values compare favorably with commercially

available fan of similar dimensions. Figure 6 shows the flow forced by this fan through configurations 2 to 5, and the corresponding handset pressure drop. Here, as expected, it can be seen that increasing the level of blockage reduces the flow rate through the handset and increases the pressure drop. The introduction of the 2.5 mm perforated plate in configuration 3 causes a 14% reduction in flow rate compared to configuration 2, whilst replacing the 2.5 mm perforations with 1.6 mm perforations causes further flow rate reduction of 34%. However, for configurations 4 and 5, when using 1 mm rather than 1.6 mm diameter perforations, the reduction in flow rate is small at only 5%.

Figure 7 shows the transient response characteristics of the phone, firstly to the heater being turned on with no fan on, and then to the fan being turned on. The time constants vary across the phone, as illustrated on the graph. The PCB and front cover had time constants of 400 s and 530 s respectively during the initial heating phase, with similar time constants during the cooling phase. During the heating phase, the back cover had a significantly longer time constant than the other locations, possibly as a result of the large thermal mass of the battery which is in close thermal contact with the temperature measurement point. The back cover time constant was significantly reduced during the cooling phase as a result of the close proximity of the forced air stream to the back cover.

Figure 8 shows the temperature rise of the phone when cooled by the fan, and also when no fan was present. The configurations considered here are numbers 1 and 2 as defined in Table 1. From figure 8 it is clear that the fan reduces the highest temperature of the phone by approximately 40%. This causes the allowable heat dissipation to increase from 1.2 W for the no fan case, to 1.9 W when cooled by the fan.

Figure 9 presents the temperature rise of the phone for varying degrees of blockages, corresponding to configurations 2, 3, 4 and 5 as defined in table 1. These blockages may be considered to correspond to minimum flow areas induced by the presence of components on the PCB. With the exception of the 2.5 mm perforations of configuration 3, it is evident that as expected, increasing the degree of blockage causes the temperature rise of the phone to increase. The increase in the allowable heat dissipation from configuration 2 to 3 may be explainable by experimental error, but could also be a result of increased thermal mixing as a

result of the formation of jet structures downstream of the holes in the perforated plates. Any gains which ensue from this thermal mixing are offset by reduced flow rate which results from the increased blockage in configurations 4 and 5. The change in allowable heat dissipation between configurations 4 and 5 is small, and this is a result of the small change in flow rate between the two configurations which was observed in figure 6.

Figure 10 looks at the effect of fan rotational speed on the temperature rise of the phone and the maximum allowable heat dissipation. The rotational speed is important in terms of power dissipation, as the power consumed by the fan is proportional to the fan speed raised to the power of three. Hence any reductions in fan speed can greatly reduce the demand on the battery. The reduction of rotational speed from 7500 to 4000 RPM resulted in a reduction in fan power consumption of approximately 15% the higher speed, whilst the reduction in the maximum allowable phone power dissipation is only 14% as it goes from 1.7 to 1.5 W, as indicated in figure 10. Hence the penalty in terms of fan power consumption of over cooling the handset is evident. Reducing rotational speed also has major benefits in terms of acoustics and reliability, two other factors that are critical to the mobile phone industry if fans are to be implemented in handsets.

The data presented in figures 8, 9 and 10 is summarized in figure 11, which presents the percentage increases in allowable heat dissipation which can be achieved by the cooled configurations 2 to 6, compared to the no fan configuration 1. From this figure it is clear that for the best case scenario of low blockage and even heat dissipation over the PCB, increases of ~ 75% can be achieved, and that for higher levels of blockage this value is likely to be in the region of 40 to 60%. It should be noted that as a result of the relatively large over estimation of the allowable heat dissipation for configuration 1 which is discussed at the end of the Experimental section, the percentage improvements in reality will be greater than those presented in figure 11.

It is clear that in order to achieve the gains which have been demonstrated, a percentage of the volume and battery power of the phone must be dedicated to the cooler, whilst a very low acoustic noise emission must be tolerated. These features, although small in magnitude, are the primary impediments to the commercial deployment of this technology. With this in mind the

authors have also developed integrated fan and heat sink solutions, not presented here, in which the magnitudes of these features are reduced, whilst performance is improved. As an example, a 130x50x22 mm handset, can dissipate 5 W of heat with the assistance of this integrated fan and heat sink technology. Thus, the deployment of miniature fan cooling technology can enable enhanced processing and download capabilities in future mobile phone applications.

CONCLUSIONS

- A custom fan was designed, manufactured and characterized. Its aerodynamic performance characteristics were found to compare favorably with commercially available fans of similar dimensions.
- When integrated into the phone the fan supplied flow rates ranging from $0.75 \times 10^4 \text{ m}^3/\text{s}$ to $1.4^4 \text{ m}^3/\text{s}$, increasing with reduced blockage.
- Thermal time constants for the handset investigated were seen to vary spatially across the handset, with proximity to thermal masses increasing the time constant, and proximity to the forced air stream reducing the time constant.
- When integrated into a mobile phone with minimal flow blockage, the fan brought about a 75% increase in allowable heat dissipation relative to a phone with no fan based on the maximum surface temperature constraint.
- In the presence of realistic blockages the increase in allowable heat dissipation relative to a phone with no fan is 40 to 60%.
- The importance of operating the fan at the lowest possible speed was observed, as reduced fan speed resulted in 15% of the power consumption, with only a 14% reduction in allowable heat dissipation.

ACKNOWLEDGEMENTS

The authors wish to acknowledge the financial support of Enterprise Ireland.

REFERENCES

1. Lin, S.-C. and C. Chou, Applied Thermal Engineering 24 (2004) 2375–2389, 2004, "Blockage effect of axial-flow fans applied on heat sink assembly." Applied Thermal Engineering **24**, pp. 2375–2389

2. Loh, C.K., D. Nelson, and D.J. Chou. 2001, "Thermal characterization of fan-heat sink systems in miniature axial fan and micro blower airflow." in *Semiconductor Thermal Measurement and Management, Seventeenth Annual IEEE Symposium*.
3. Tan, F.L. and C.P. Tso, 2004, "Cooling of mobile electronic devices using phase change materials." *Applied Thermal Eng.*, **24**(2-3), pp. 159-169.
4. Launay, S., V. Sartre, and M. Lallemand, 2004, "Experimental study on silicon micro-heat pipe arrays." *Applied Thermal Eng.*, **24**(2-3), pp. 233-243.
5. Walsh, E.J., Walsh, P., Grimes, R., Egan, V., 2008, "Thermal management of low profile electronic equipment using radial fans and heat sinks", *ASME J. of Heat Transfer*, vol. 130, 12, 125001-1-8.
6. Walsh, E.J. and R. Grimes, 2007, "Low profile fan and heat sink thermal management solution for portable applications." *Inter. J. of Thermal Sciences* 1182-1190, **46**, pp. 1182-1190.
7. Egan, V., Walsh, P., Walsh, E., Grimes, R, 2009, "Thermal Analysis of Miniature Low Profile Heat Sinks With and Without Fins", *ASME J. of Elec. Pack.*, vol. 131, 3, doi:10.1115/1.3144150.
8. Egan, V., Stafford, J., Walsh, P., Walsh, E., 2009, "An experimental study on the performance of miniature heat sinks for forced convection air cooling", *ASME J. of Heat Transfer*, vol. 131, 7, 9 pages, doi:10.1115/1.3110005.
9. Stafford, J., Walsh, E.J., Egan, V., 2009, "Characterizing convective heat transfer using quantitative heated-thin-foil thermography", *Meas. Sci. Technol.*, vol. 20, 11 pages, doi:10.1088/0957-0233/20/10/105401.
10. Grimes, R., et al., 2005, "The Effect of Geometric Scaling on Aerodynamic Performance." *AIAA Journal*, **43**(11), pp. 2293-2298.
11. Walsh, P., Egan, V., Grimes, R., Walsh, E., 2009, "Profile Scaling of Miniature Centrifugal Fans", *Heat Transfer Engineering*, vol. 30, 1-2, pp. 130-137, DOI: 10.1080/01457630802293555.
12. Walsh, E.J., Walsh, P.A., Punch, J. & R. Grimes, 2009, "Acoustic emissions from active cooling solutions for portable devices", *IEEE Transactions on Components and Packaging Technologies*, Vol. 32, 4, pp. 776-783.

13. Walsh, E.J., Walsh, P.A., Grimes, R. and J. Punch, 2008, “Acoustic emissions from active cooling solutions for portable devices”, Proceedings of ITHERM 2008, pp. 464-470, 28th – 31st May, Orlando, Florida, USA.
14. Holman, J.P., 1992, Heat Transfer, 7th Edition, McGraw Hill, London.

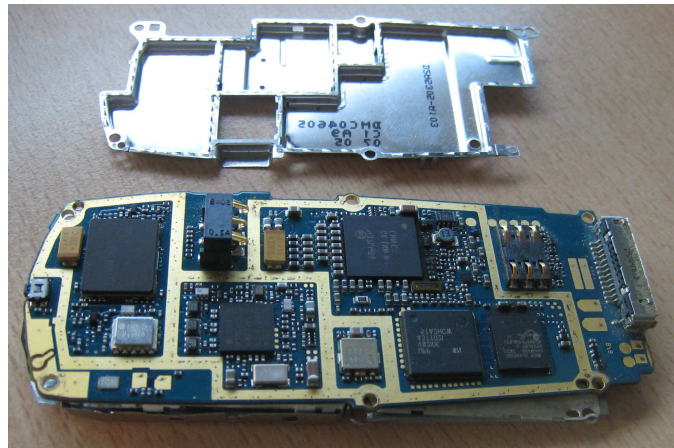
Table 1. Summary of phone test configurations.

| Configuration | Fan Power consumption (mW) | Fan speed (RPM) | Perforated plate |
|---------------|----------------------------|-----------------|------------------|
| 1 | - | - | None |
| 2 | 59 | 7,500 | None |
| 3 | 59 | 7,500 | 2.5mm holes |
| 4 | 59 | 7,500 | 1.6mm holes |
| 5 | 59 | 7,500 | 1.0 mm holes |
| 6 | 26 | 4,000 | 1.6mm holes |

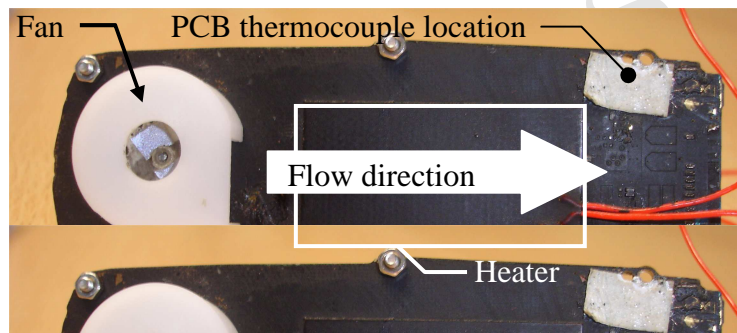
Table 2. Values used to estimate the error incurred in calculation of allowable heat dissipation as a result of assuming constant case to ambient thermal resistance

| Configuration | T_{∞} (°K) | $T_{c-\infty_A}$ (°K) | $T_{c-\infty_t}$ (°K) | $T_{h-\infty_t}$ (°K) | ϵ_c | e (%) |
|---------------|-------------------|-----------------------|-----------------------|-----------------------|--------------|-------|
| 1 | 293 | 15 | 25.6 | 30.8 | 0.9 | 9 |
| 3 | 293 | 15 | 15 | 18.5 | 0.9 | 0 |

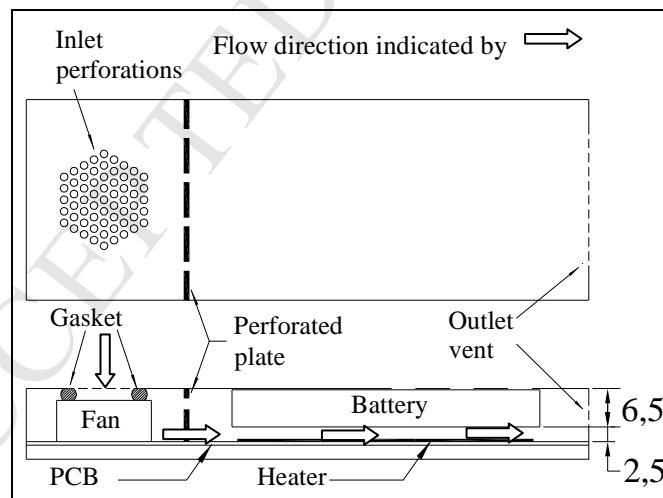
**Figure 1.** Nokia 3120 mobile phone in which the performance active cooling solutions was tested.



(a)



(b)



(c)

Figure 2. (a) Nokia 3210 populated PCB and metal cover sheet (b) PCB with components removed and replaced with fan and heater (c) schematic of phone with fan, battery, gasket, heater and inlet and outlet vents. Note that the inlet to the fan is machined into the back cover, and that the vents were machined into the original phone cover.

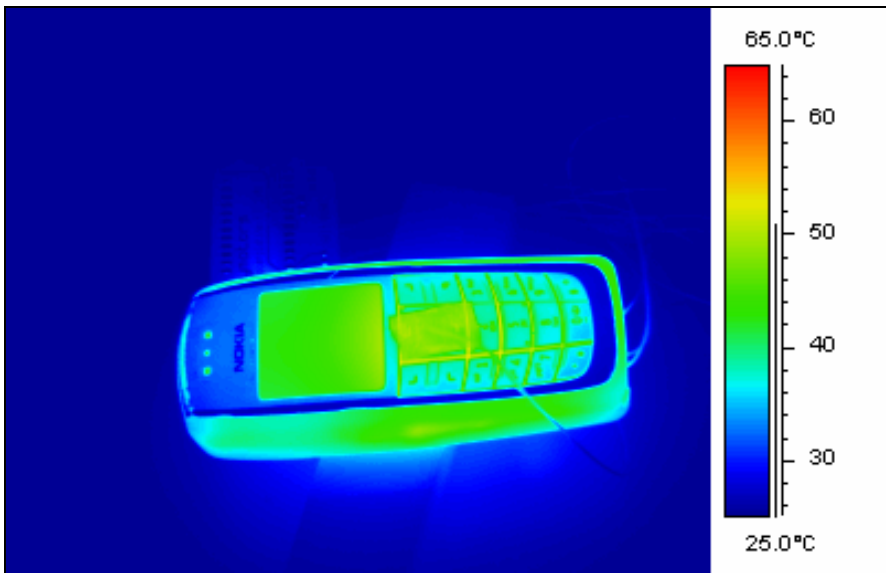


Figure 3. IR image used to locate point of maximum temperature on front surfaces of the phone.

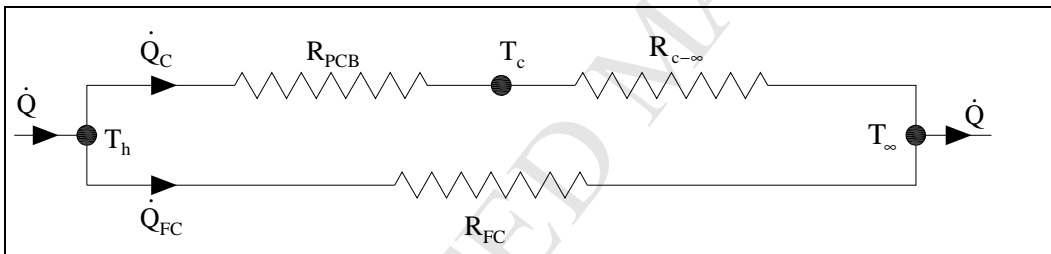


Figure 4. Simplified thermal resistance network representing the heat flow path from source to ambient.

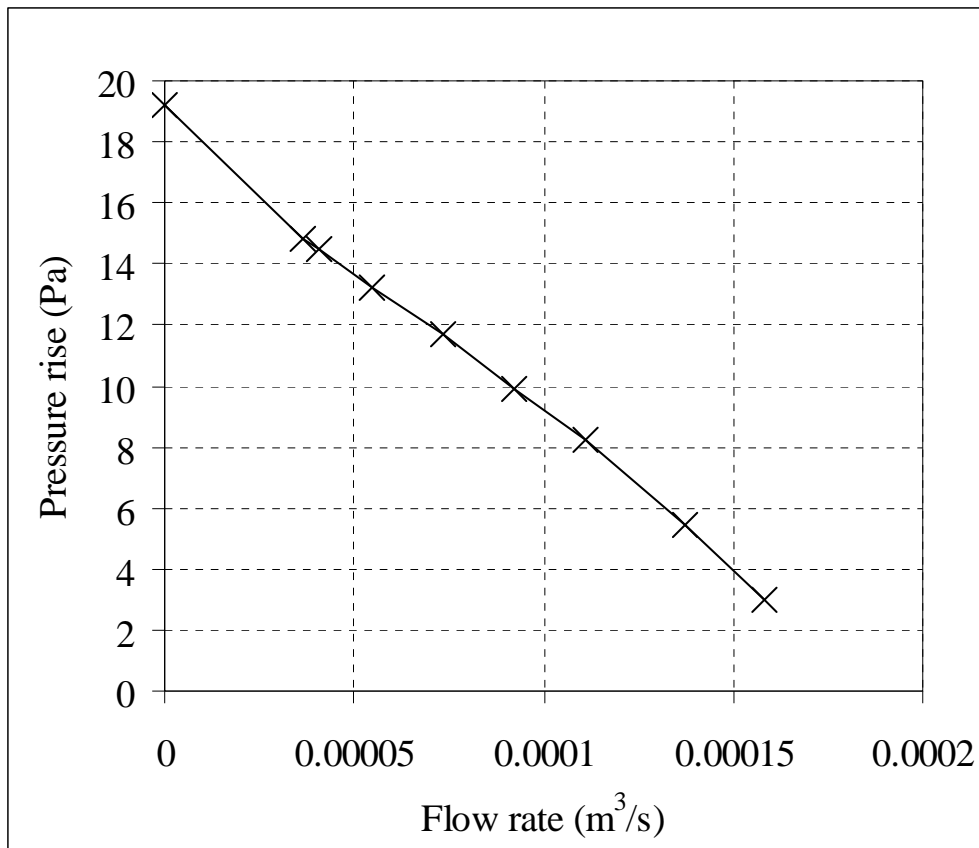


Figure 5. Fan performance curve measured at a rotational speed of 7500RPM.

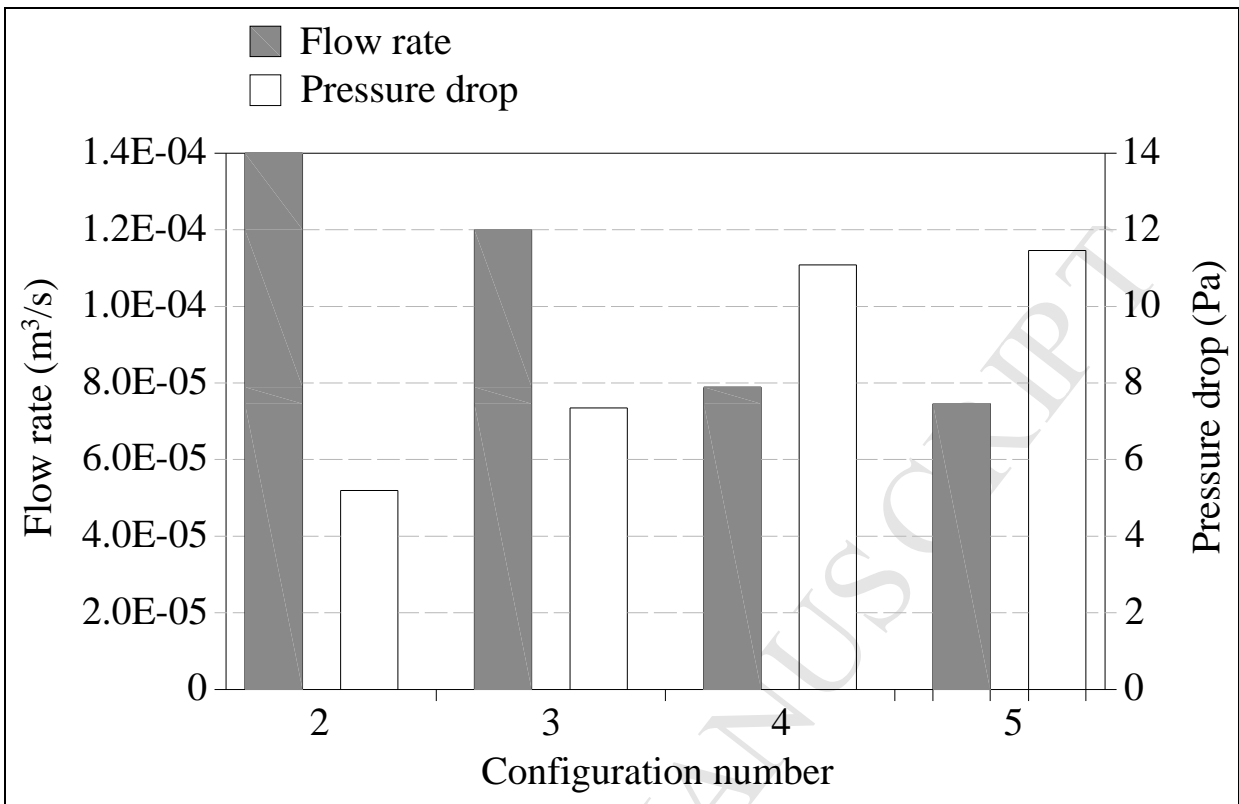


Figure 6. Flow rate and pressure drop in the handset for configurations 2 to 5.

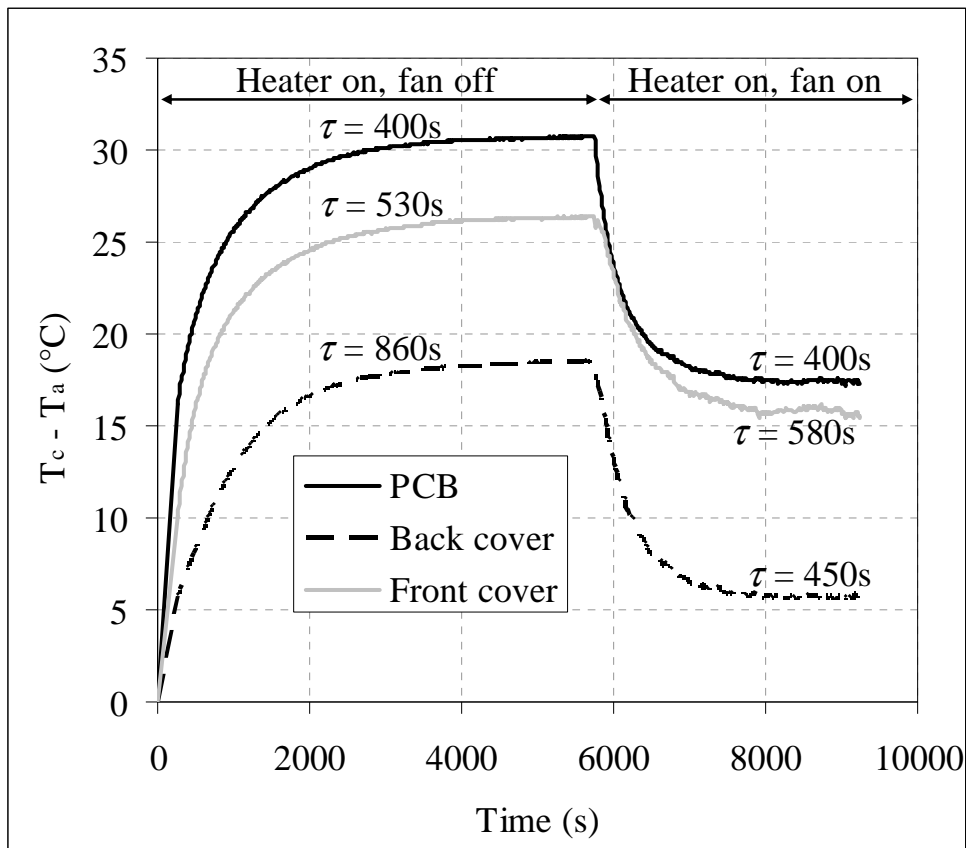


Figure 7. Thermal response of phone to initial step input of heat with no fan, and the response to the fan being turned on under the conditions of configuration 2.

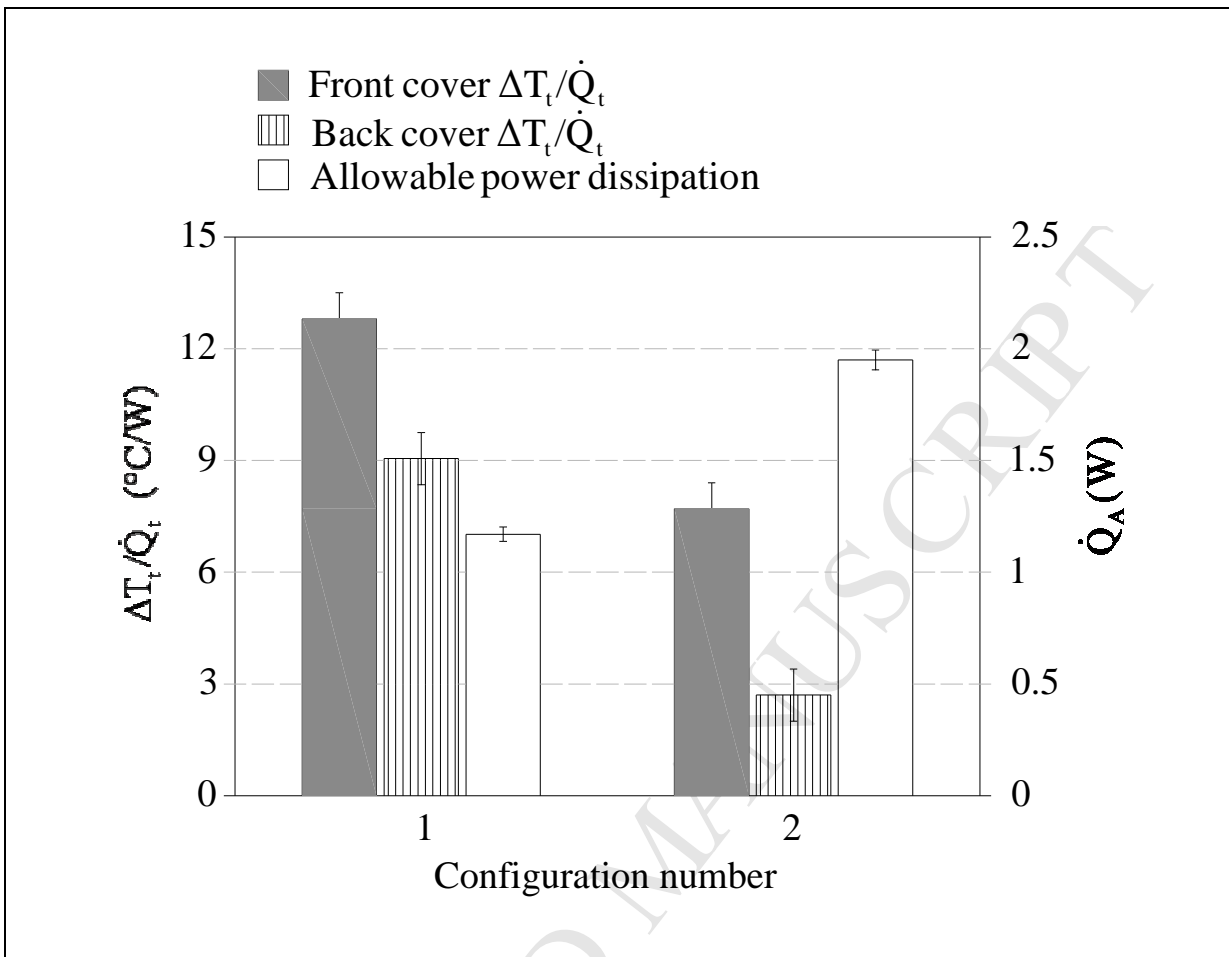


Figure 8. Temperature rise above ambient per watt of heat dissipated, and allowable heat dissipation for no fan and a custom fan at rotational speed of 7500RPM. See Table 1 for definition of test configurations.

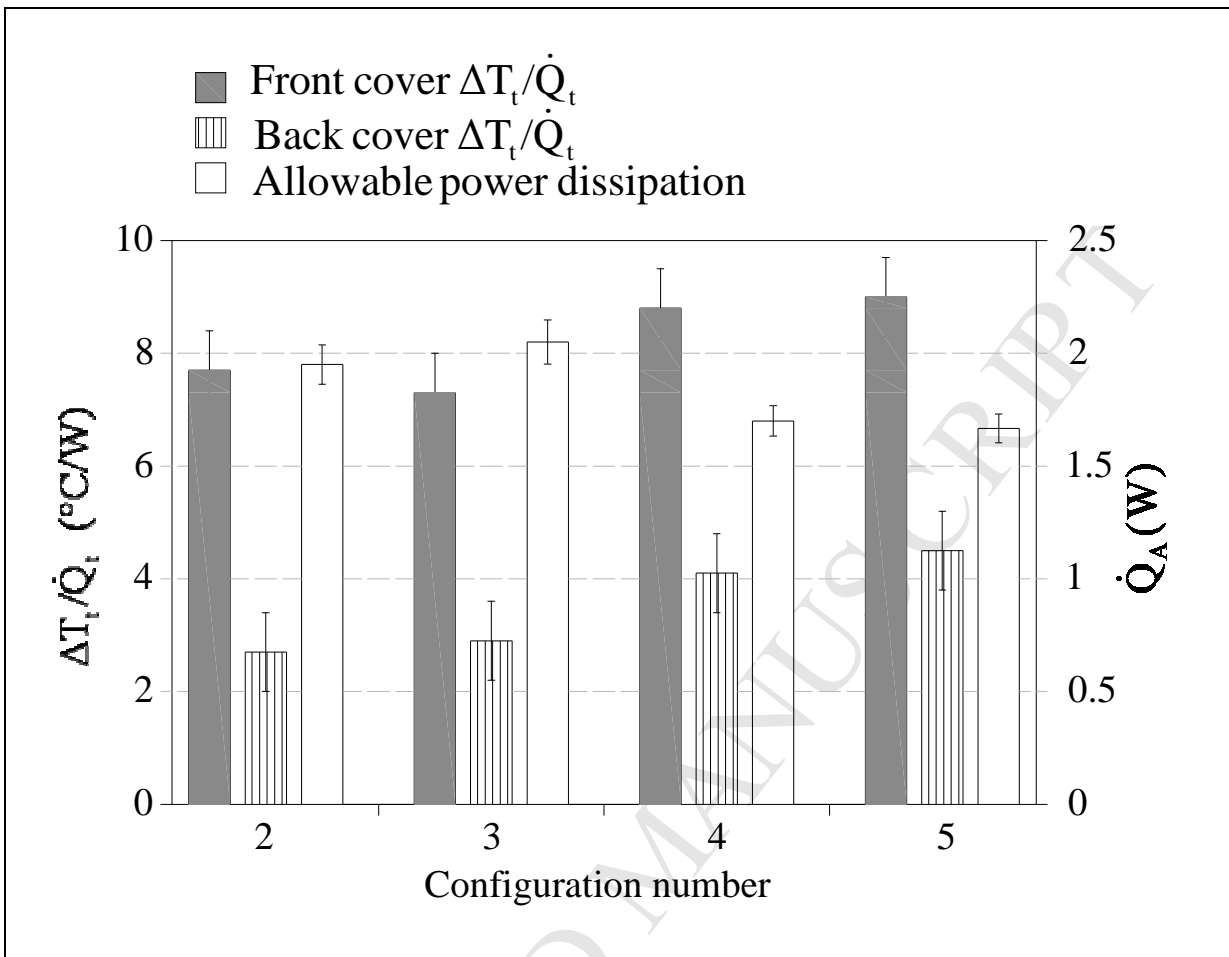


Figure 9. The effect of blockage on the temperature rise of the phone casing and the maximum allowable heat dissipation for the case of the custom fan design. See Table 1 for definition of test configurations.

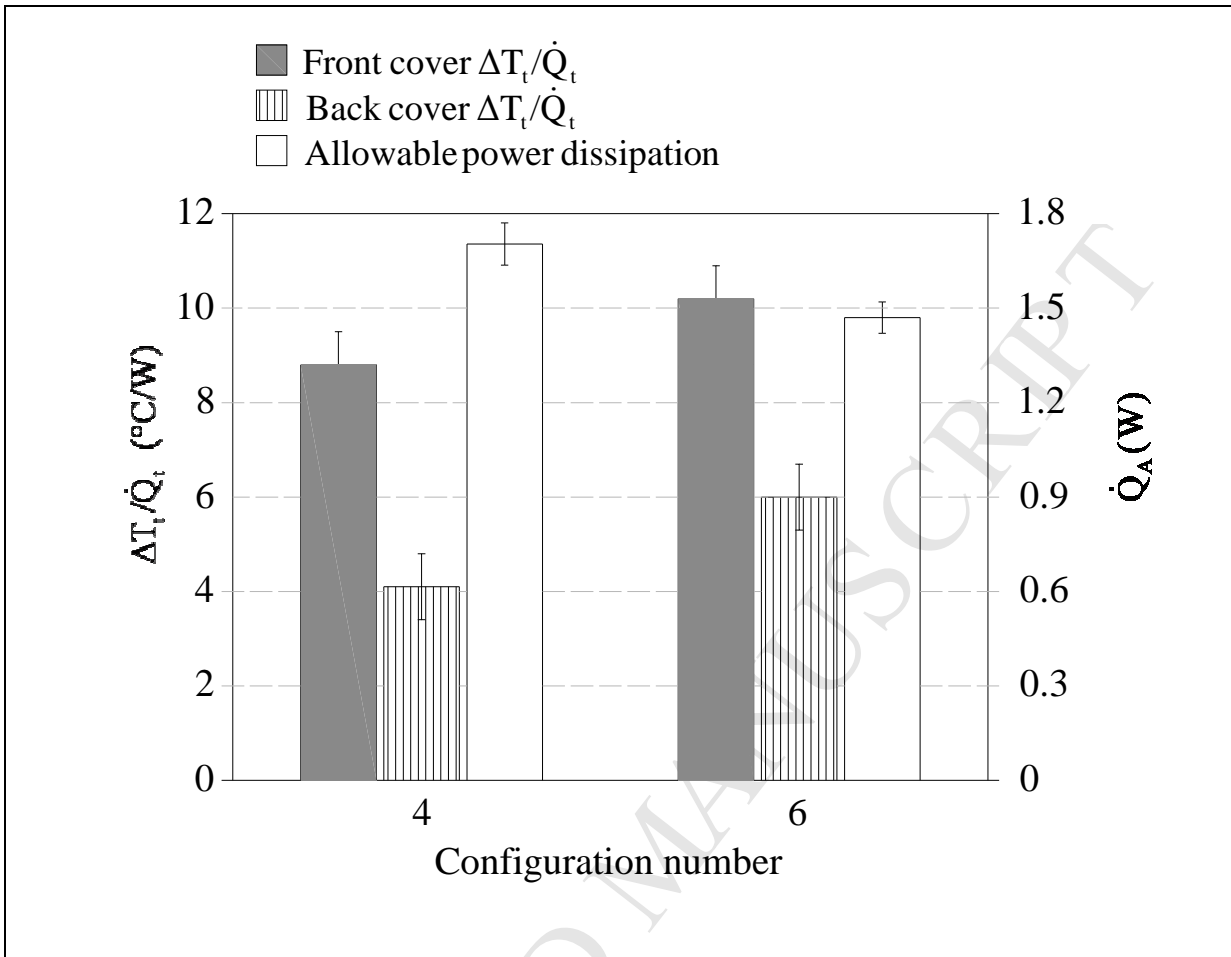


Figure 10. The effect of rotational speed on the temperature rise of the phone casing and the maximum allowable heat dissipation for the case of the custom fan design. See Table 1 for definition of test configurations.

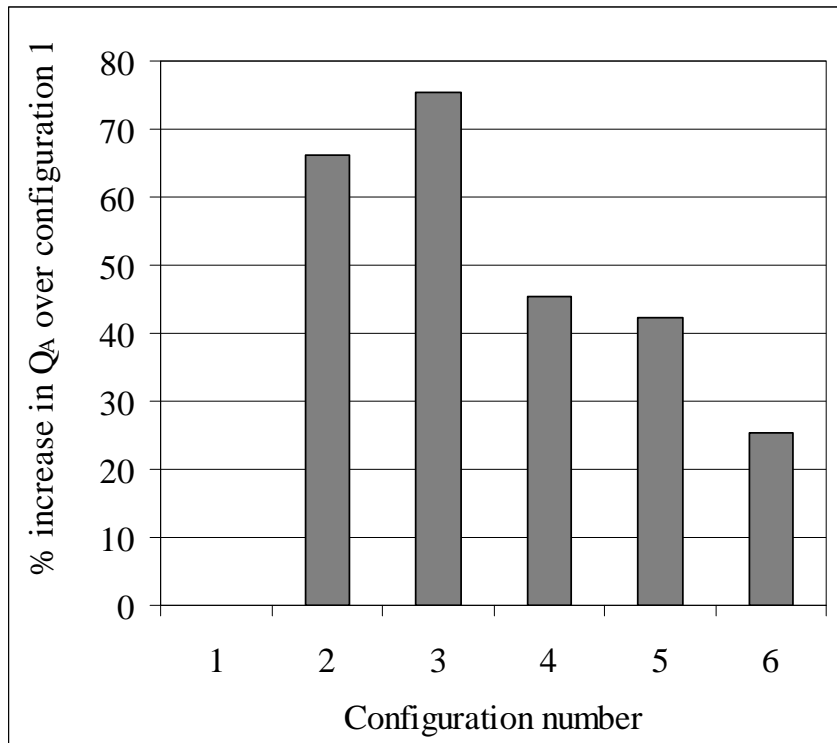


Figure 11. Percentage gains in allowable heat dissipation which are achievable compared to the no fan configuration 1.